ZJUI ECE 445

Senior Design Project

FINAL REPORT

SMART POWER ROUTING WITH MPPT-BASED WIND TURBINE

Project #19

Rong LI
郦　融
rongli3@illinois.edu

Tiantian ZHONG
钟天天
tzhong7@illinois.edu

Zhekai ZHENG
郑哲楷
zhekaiz3@illinois.edu

TA: Bohao ZHANG (张博昊)
Sponsor: Prof. Lin QIU (邱　麟)

June 1, 2024

Acknowledgement

With the sincerest gratitude, we would like to thank everyone who were involved in the development of the project for their intelligence and effort.

We thank our sponsor, Prof. Lin Qiu, for his directions on implementing the solution.

We thank our teaching assistant, Mr. Bohao Zhang, for his understanding and support in the project.

We thank the teammates, Mr. Rong Li, Mr. Tiantian Zhong, and Mr. Zhekai Zheng, for their dedication to this project for the past four months, and for their effort on implementing the solution and pursuing the completeness of the project.

We thank Call of Duty 19: Modern Warfare II – "the first COD for the youngs." And, we thank The Finals, who has accompanied the team members for months and provided unimaginable emotional support and entertainment.

Though graduation separates us, we wish to meet each other one day in the future.

Abstract

For hundreds of years, human beings have been using wind power as energy source. In the recent centuries, human beings are able to produce electricity from wind power. While this power of nature provides an alternative source of electricity for residents in undeveloped regions, a power router is needed to switch the power output to a backup source for better stability in power supply. This project provides a solution to convert wind power to electricity using a modular multilevel converter (MMC), and adds an STM32-based power router to handle overload and underload detection, and switch between wind power and the available backup power based on output voltage to ensure a stable power output. A LCD-based user interface is developed to provide visual indication of the system status, and an Android mobile app is implemented to allow complete control of the routing system based on Message Queueing Telementary Transport (MQTT) with an on-board WiFi receiver/transmitter module ESP-12F.

Keywords: Modular Multilevel Converter, AC/DC Conversion, Embedded System

Contents

1   Introduction

1.1   Problem Statement

In 2023, China's wind power installed capacity reached 441.34 gigawatts, accounting for 15.11% of the total installed capacity for power generation, with a year-on-year increase of 20.7% [1]. This growth trend underscores the escalating demand for wind energy as a renewable power source. Moreover, there's a growing interest among ordinary consumers in small-scale wind power solutions, driven by a desire for decentralized energy generation and environmental sustainability.

However, challenges persist in the wind power sector, including issues of low stability inherent to wind energy, the substantial land footprint required by traditional large-scale installations, and the high maintenance costs associated with such setups. These drawbacks highlight the pressing need for innovative solutions that address the reliability and cost-effectiveness of a small-scale wind power generation system, particularly in the context of smaller, more accessible systems tailored to meet the evolving needs of diverse user groups.

Therefore, the project aims to design a small-scale wind power generation system with power routing functionality. This entails creating a compact and efficient system capable of harnessing wind energy while incorporating mechanisms to seamlessly switch between power sources to ensure an uninterrupted electricity supply. Key objectives include maximizing power output, enhancing system reliability, and optimizing energy management for diverse applications.

1.2   Solution Overview

The envisaged solution endeavors to furnish a comprehensive apparatus of appropriate dimensions tailored to furnish electrical power to consumers residing in regions characterized by significant wind activity. Comprising pre-assembled wind turbine apparatus, a power rectification module facilitating AC-DC conversion, and a suite of controllers facilitating maximum power point tracking (MPPT) and safety protocols, this solution is poised to address the exigencies of reliable and efficient power generation.

Moreover, a power routing mechanism is envisaged to seamlessly transition to an alternative power source in the event of wind turbine malfunction. Augmenting operational transparency, a user interface is incorporated to furnish real-time data encompassing voltage, current, and power source statuses. Additionally, to bolster safety protocols, supplementary fusing mechanisms and emergency shutdown functionalities are meticulously integrated into the design paradigm.

1.3   Visual Aid

The visual aid shows the components and their interconnections, which demonstrates the top-level design of the solution. It is shown in Figure 1.1.

1.4   High-Level Requirements

For the final implementation of our solution, the following high-level requirements must be satisfied:

1. The system must be able to deliver stable DC voltage greater than 8 V (with ripple less than ±10%) and current up to 10 A. The maximally allowed voltage and current are customizable by the user.

2. The system must be able to provide a local and remote user interface. The local user interface should indicate the basic status of the system (power on/off, running normally / in fault, WiFi connected/disconnected, backup power in use/standby/fault.)

3. The system must disconnect its output within 1 s when the wind power and the backup power when current delivered to the load exceeds 10 A.
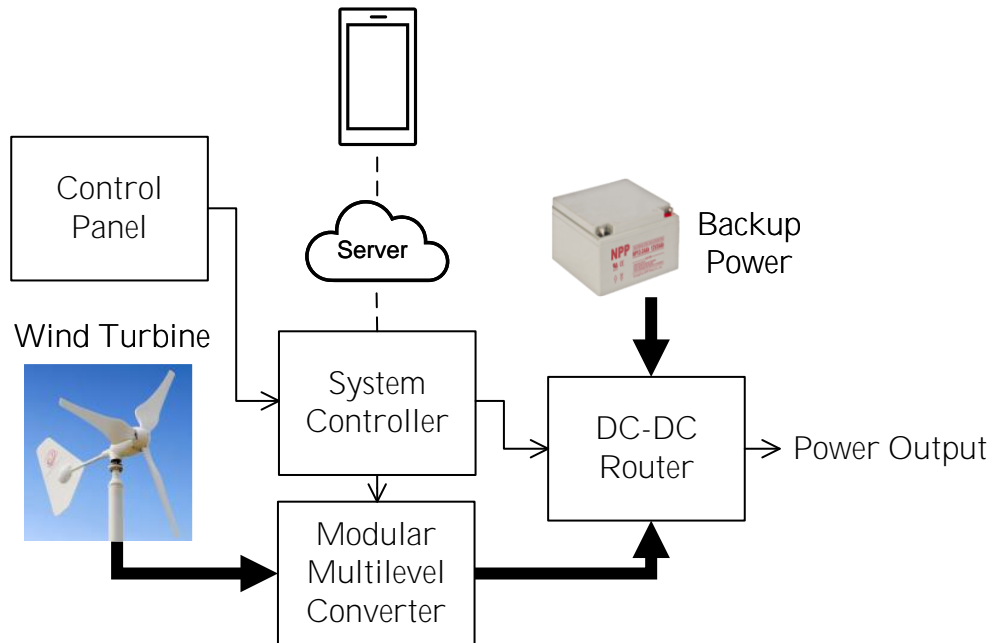

Figure 1.1   The visual aid of the solution.

2   Design

The design of the system can be broken into three major parts. The power transmission module converts wind power to electricity and directs it to the users. The power routing module connects the output to the backup power source or the MMC based on the necessary power needed for the load. The system controller module processes the user interface, monitors the status of the system, and assures the safety of the system. Figure 2.1 presents the block diagram of the system.

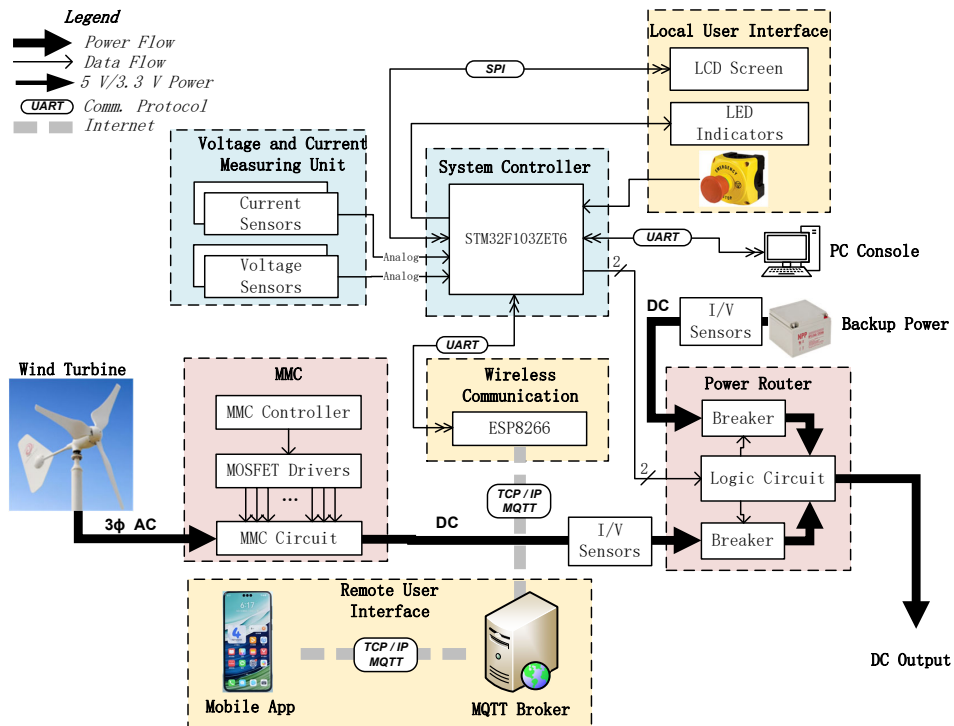All Requirements and Verification Tables (R&V Tables) are listed in Appendix **??**.

Figure 2.1 The block diagram of the system.

2.1   Wind Turbine

The primary power source of the system is a horizontal-axis wind turbine, which is connected to the Modular Multilevel Converter (MMC, to be discussed in §2.2 and Chapter **??**). It has eight blades and could automatically turn to the direction of wind. Table 2.1 lists the parameters of the wind turbine.

Table 2.1   Parameters of the Wind Turbine

Item	Parameter
Rated Voltage	24 V
Rated Power	200 W
Rated Speed	950 rpm
Startup Wind Speed	1.5 m/s

Figure 2.2   The horizontal-axis wind turbine.

2.2   Modular Multilevel Converter

The Modular Multilevel Converter (MMC) is a AC-DC/DC-AC conversion technology conventionally used in High Voltage Direct Current (HVDC) transmission. The team tries to verify the feasibility of this technology in low-power scenarios and test its performance in this project.

The MMC is the key component of AC-DC conversion between the wind turbine and the user end. It automatically traces the maximum power point and adjust the output voltage, so as to maximize the efficiency of the wind turbine. While the circuit topology of an MMC is simple, the control algorithm poses a major challenge to the team. Figure 2.3 illustrates the circuit design of the MMC.
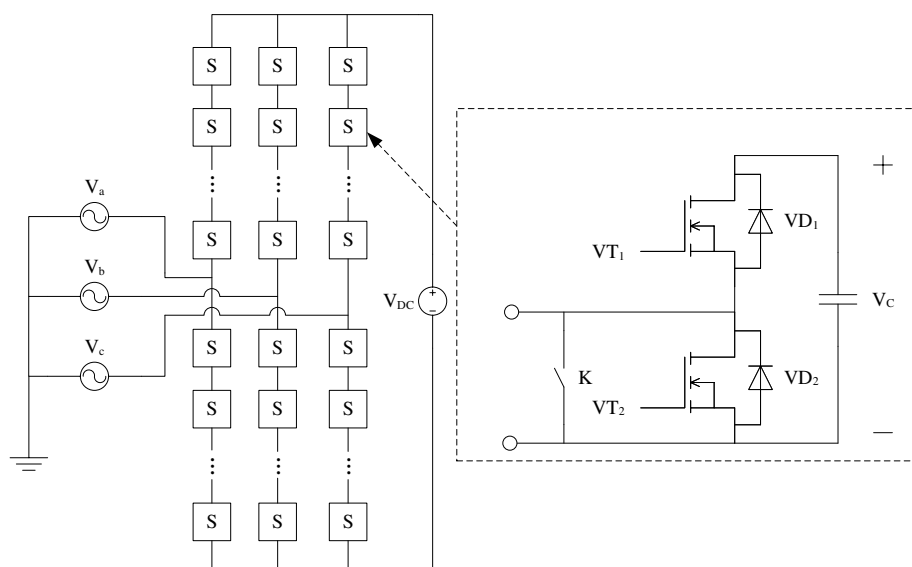

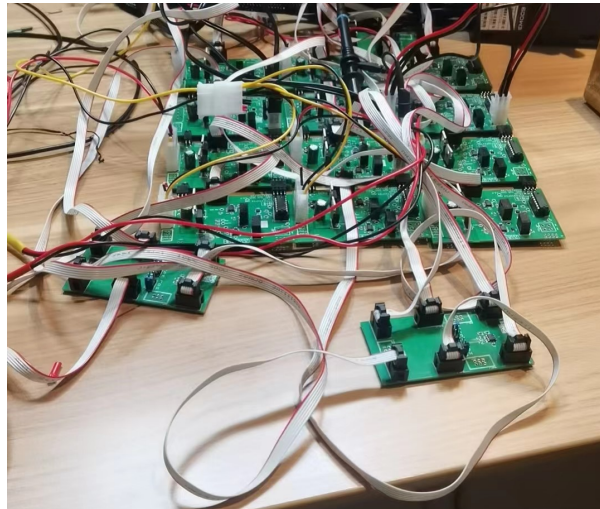**Figure 2.3**   The circuit of a modular multilevel converter.

Figure 2.4   The photo of the assembled MMC.

2.3   Power Router

The power router is designed to switch between the MMC module and the backup power supply. It is composed of four electromagnetic relays and their accessory circuit, which can be controlled by the control part signal. When the back-up signal is high, the power router will switch to the backup power supply by give high voltage to the certain relay. When the MMC signal is high, the power router will switch to the MMC module.

The two relays, shown in Figure 2.5, are used to switch the power source between the MMC and the backup power supply. When it receive the signal from the system controller, the high voltage will be given to the triode and connect the low side of relay to the ground, then the relay will close. A diode is also used to protect the relay from the reverse current. The power router is designed to handle a maximum power of 200 W and a maximum voltage of 24 V.
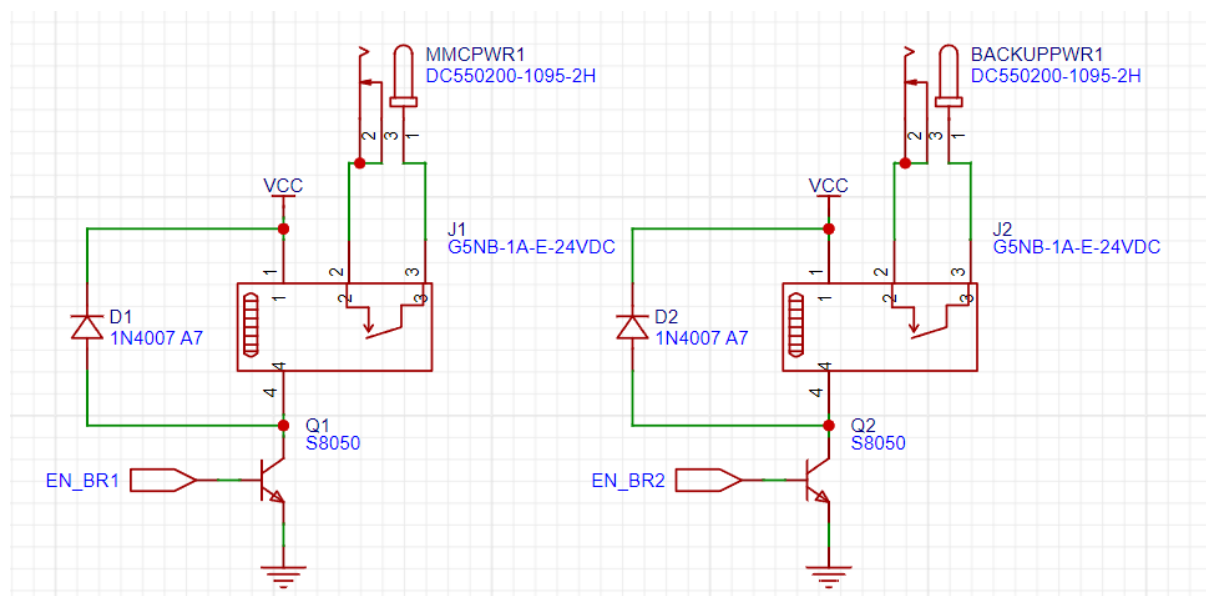

Figure 2.5   The two relays.

2.4   Voltage and Current Measuring Unit

The Voltage and Current Measuring Unit (VCMU) is designed to measure the voltage and current. The voltage sensor is composed of a voltage divider and voltage follower. The voltage divider is used to measure the output voltage of the MMC module, the back up power and the output of the system, the divider is also shown in Figure 2.7. Then the follower is used to match the impedance to the following ADC in the control part, which is shown in Figure 2.6. The maximum input voltage is 30 V, and the voltage divider is designed to convert the input voltage to 3 V to match the input voltage of the control part.

2.4.1   Current and Voltage Sensors

The current measurement is composed of a current sensor chip, which is shown in Figure 2.8, and its accessory circuit. The current sensor is used to measure the current and change it to output voltage. Here we use existing MT9523CT-20BF5, which is a Hall effect-based linear current sensor chip and could measure up to 20 A DC current. The voltage output of the chip has a linear relationship with the current,

$$V_{meas,I} = V_{cc}/2 + I \times 100 \, \text{mV/A}. \tag{2.1}$$

Here we use $V_{cc} = 5$ V. The circuit of the current sensor is shown in Figure 2.9.

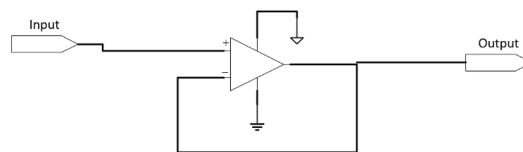**Figure 2.6**   The voltage follower.
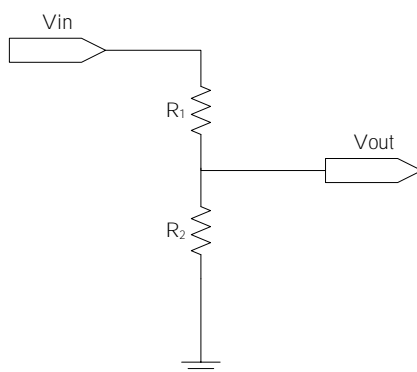

Figure 2.7   The voltage divider.

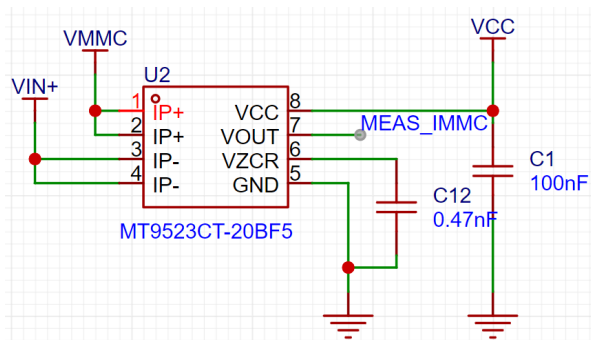**Figure 2.8**   The current sensor chip.

Figure 2.9   The circuit of the current sensor chip.

2.5   System Controller

The system controller is designed to provide support functions including generating PWM control signals for the DC/DC converter, processing user interface, and providing safety measures. By reading the voltage and current info from VCMU, it delivers real-time power information to the user interfaces and controls DC/DC converter by adjusting the duty ratio of the PWM signal. Connected to a wireless communication module, it also allows the users to monitor the system status and send instructions. To maximize the efficiency of MCU computing resources, FreeRTOS [2] is introduced to provide multi-task processing.

2.5.1   Hardware Design

The controller is integrated into the motherboard of the system, which is composed of a minimal system of STM32F103ZET6, an ESP-12F Wi-Fi module manufactured by Ai-Thinker, LEDs indicating system status (also called the Local User Interface; see §2.7), and ports to connect the motherboard to other modules of the system. Figure 2.10 shows the PCB design of the system controller board, or the mother board.
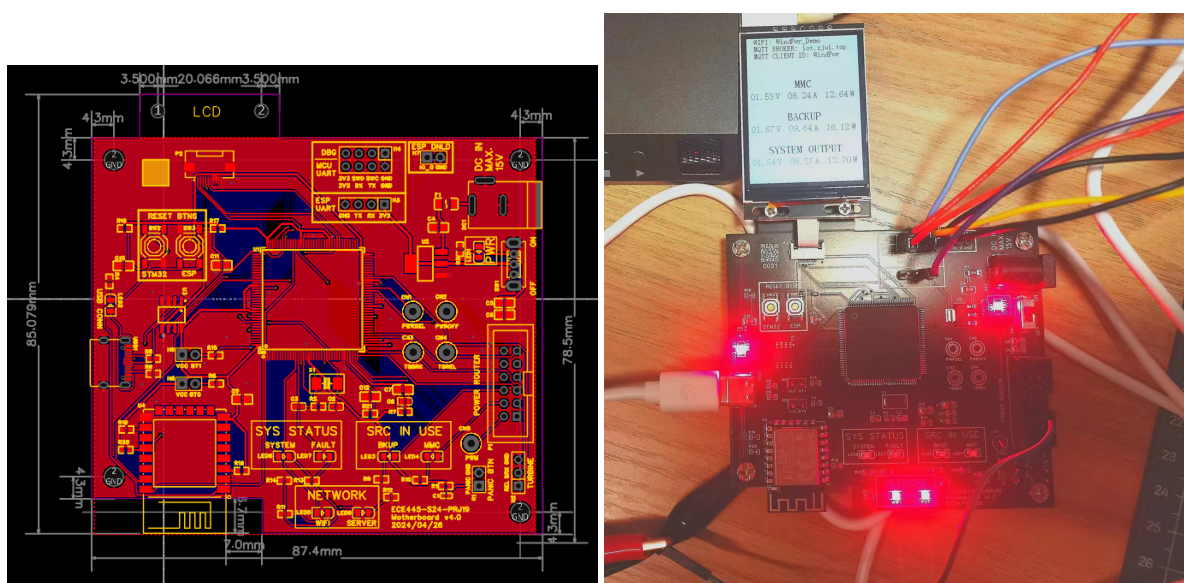

Figure 2.10   Left: The PCB design schematic of motherboard. Right: The photo of the motherboard PCB.

2.5.2   Software Design

The STM32 is programmed using FreeRTOS with CMSIS-RTOS API. The FreeRTOS handles multitasking and allows different tasks to be performed in parallel. The tasks communicate with each other using message queues. Figures 2.11 and 2.12 demonstrates the architecture of the FreeRTOS-integrated system.
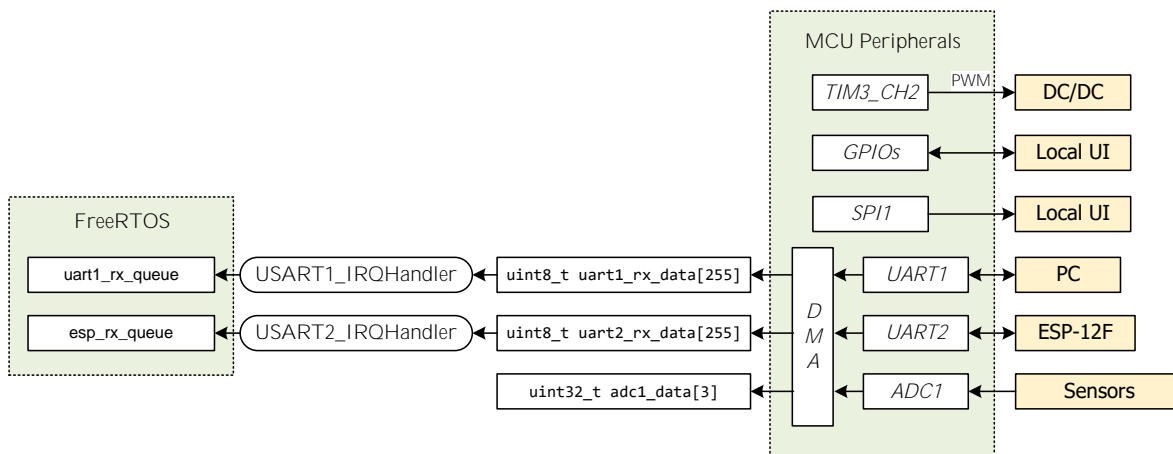
Figure 2.11   The peripherals and the IRQ functions of the MCU.
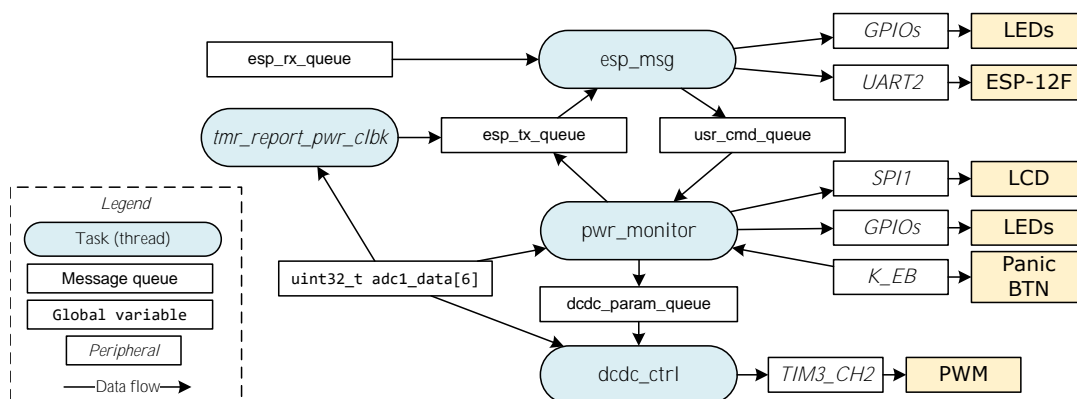
Figure 2.12   Tasks and message queues of FreeRTOS.

2.6   Wireless Communication

The wireless communication subsystem aims to transmit data between the system and the user client app, which is composed of an ESP-12F module and an MQTT server. (See) This subsystem works according to instructions received from its serial port and can transmit data between MQTT servers and itself. Equipped with a Wi-Fi MCU designed by ESPRESSIF, the ESP-12F supports 2.4 GHz WiFi communication and can be driven using AT instruction set [3], [4]. The AT supports easy connection to WiFi hotspots and MQTT server [4], which eases the development of this project.

The MQTT server used in the project is an Aliyun Simple Application Server with Ubuntu 20.04, which provides MQTT messaging services through the open-source version of EMQX software [5]. Note

that MQTT is selected to be our desired protocol because of its lightweight, efficiency, and the nature of bi-directional communications [6].

   As is mentioned in §2.5, the wireless communication subsystem is the key to delivering system information to the users. It should pack real-time power delivery, source connected to the power output, MMC status and backup power status together and deliver it to the MQTT server at topic `system/status`. It is also expected to listen to topic `usr/cmd` to catch any user instructions including power on/off. Figure 2.13 shows the circuit of the wireless communication module, and Table 2.2 shows the MQTT topics and their functions.
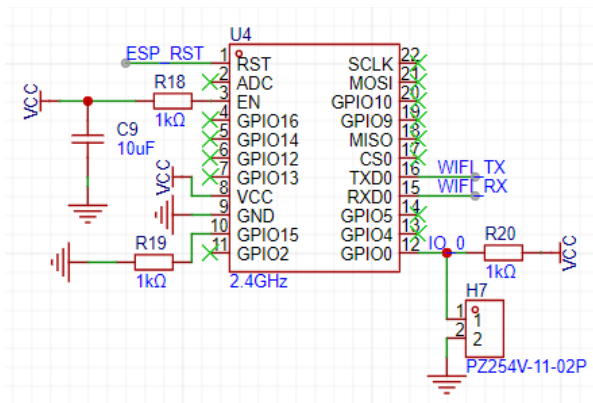

Figure 2.13   The schematic of wireless communication module.

Table 2.2   MQTT Topics and Their Functions

Topic	QoS	Function
system/status	0	Real-time power of sources and system output
system/warning	2	Warning information of the system.
usr/cmd	2	User instructions.
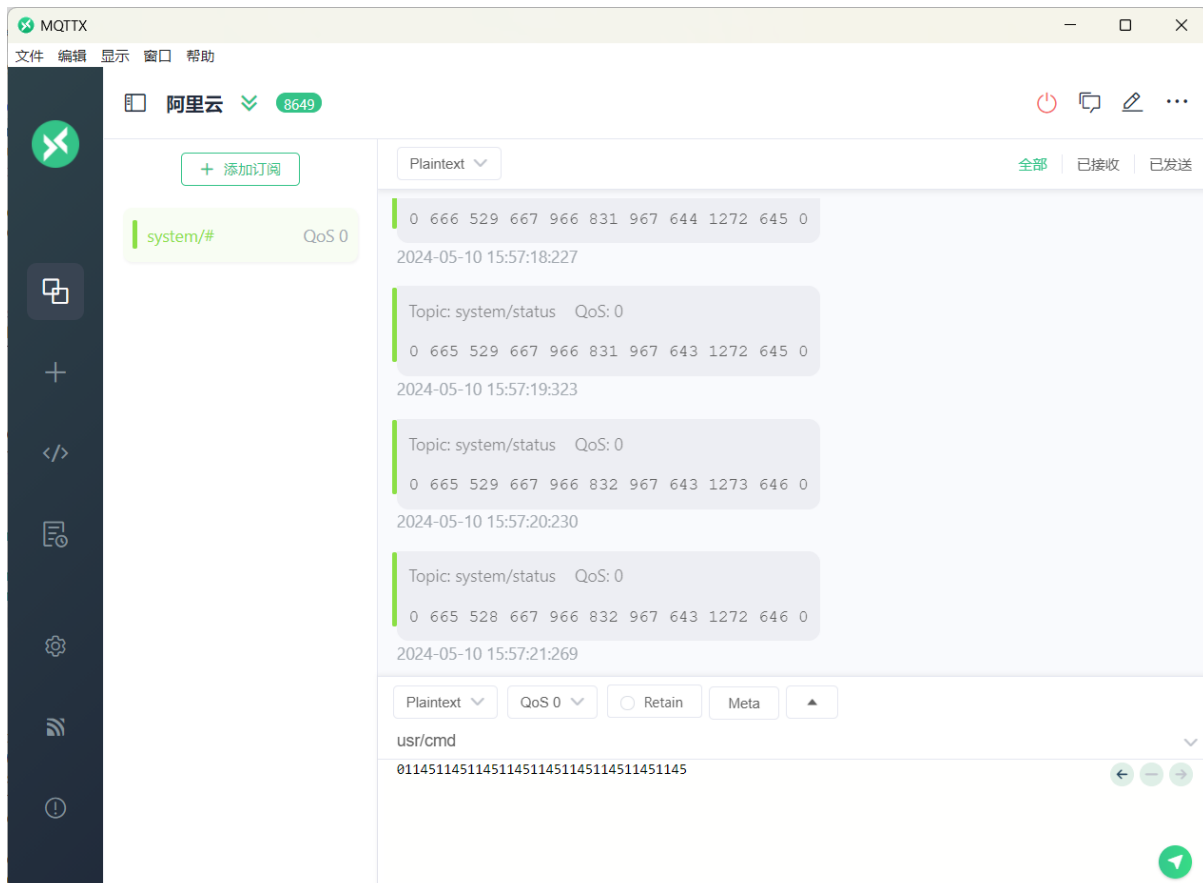
Figure 2.14   The demonstration of the motherboard sending MQTT message.

2.7   Local User Interface

The Local User Interface (LUI) is a control panel connected to the system controller through wires. It contains a set of buttons and LEDs that allow users to perform basic operations on the system and be informed of its status. It also contains a panic button which could cut off all power sources and stop the turbine to avoid any disasters.

The LUI is integrated to the system motherboard, which is shown in Figure 2.10.

2.8   Remote User Interface

The Remote User Interface (RUI) is composed of an MQTT server on Aliyun and an Android app. The MQTT server allows message exchange between the system and the remote user client, so users can control and monitor the system without approaching the wind turbine. While the architecture of the RUI is shown in Figure 2.15, the following sections will explain the two major components of this subsystem.

2.8.1   MQTT Server

The MQTT server (or the broker) is deployed on the cloud, which receives and broadcasts the messages from and to clients connected. The protocol, Message Queuing Telemetry Transport (MQTT) is a lightweight publish/subscribe messaging protocol that is often used for machine-to-machine (M2M)

or Internet of Things (IoT) communications. It is designed to be efficient and reliable, even in situations with limited bandwidth or unreliable network connections [6]. MQTT allows devices to exchange messages with a broker, which then distributes those messages to any clients that subscribe the relevant topics. This makes it a popular choice for connecting and controlling remote devices, such as sensors and actuators, in various applications. Table 2.3 shows the parameters of the server we rented to deploy the MQTT broker.

Table 2.3   Parameters of the MQTT Server

Item	Parameter
Internet Bandwidth	3 Mbps
Memory	2 GB
OS	Ubuntu 20.04
MQTT Message Platform	EMQX
Supported Protocol Version	MQTT 5.0

2.8.2   Mobile App: PowerPeek

"PowerPeek" is designed to allow users to interact with the system on their mobile phones without approaching the wind turbine. As the wind turbine is placed outdoors, it is often difficult to approach especially under bad weather. Therefore, designing a mobile app is a more convenient way to demonstrate the system information to the users while keeping them from being exposed to the danger of bad weather and the risk of being hurt by the blades.

This app will be implemented using MIT App Inventor [7] with MQTT extension from Ullis [8]. The layout of PowerPeek should look like Figure 2.16.
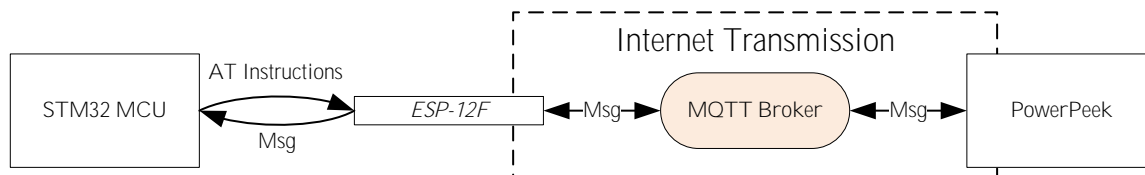

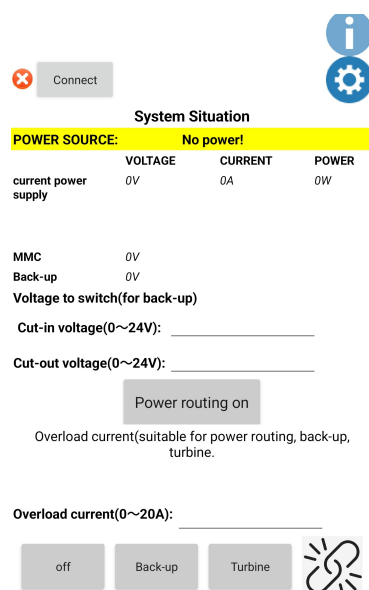**Figure 2.15**   Architecture design of PowerPeek.

Figure 2.16   UI design of PowerPeek.

2.9   Modular Multilevel Converter

The Modular Multilevel Converter (MMC) is the most important design of this project, as it transforms wind power into electricity. First raised by R. Marquart in 2011, this technology was originally designed for High Voltage Direct Current Transmission [9]. Though MMC is designed for HVDC, the team still attaches great importance to its potential for convenience in maintenance due to its nature to be modular. The functionality and efficiency of the MMC are the most important factors in the success of this project. In this chapter, the circuit topology of the MMC will be discussed and the nearest level control (NLC) algorithm will be introduced. The simulation results are also demonstrated to show the validity of the select control algorithm.

2.9.1   MMC Topology

According to [9], MMC is composed of a cascading connection of a number of converter submodules to obtain voltage waveforms having high quality, which is shown in Figure 2.17. In this project, we put six submodules on each phase, three on each branch. Each branch is connected to one phase of the output of the wind turbine.

A submodule of MMC is composed of two semiconductor switching devices (Q_1 and Q_2) and a capacitor. The status of Q_1 and Q_2 controls if the capacitor is connected to the converter in series or bypassed. Figure 2.18 illustrates a typical MMC submodule.

Referring to [10], [11], a single submodule has three states: the ON state or *inserted* state, the OFF state or *bypassed* state, and the *blocked* state, as are demonstrated in Figure 2.19. The submodule changes its working state with VT_1, VT_2, and K. The relationship is listed in Table 2.4.

13
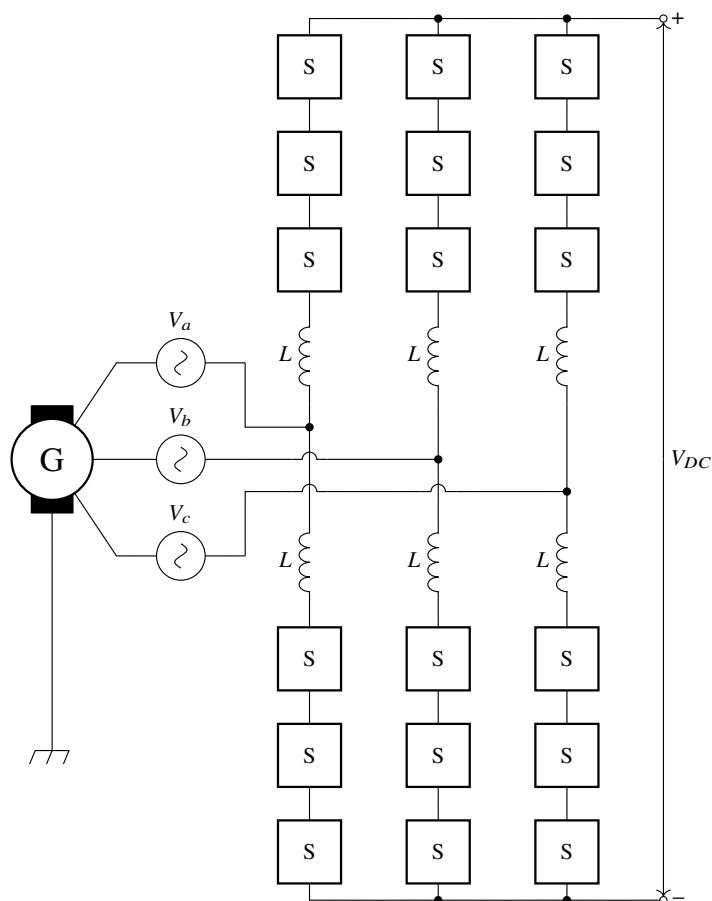
Figure 2.17   The topology of a typical MMC.
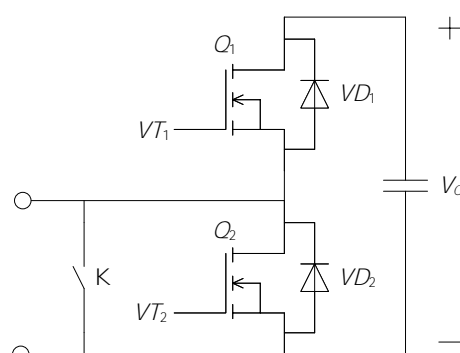
Figure 2.18   The MMC submodule.

The ON State   In this state, VT_1 is set to high and VT_2 to low, which turns the upper IGBT on and lower IGBT off, allowing current to flow through the capacitor. The capacitor is charged or discharged with the change of the terminal voltage of the submodule, i.e. $V_S = V_C$.

The OFF State   In this state, VT_1 is set to low and VT_2 to high. The capacitor is bypassed by this IGBT configuration, and the voltage across the submodule becomes $V_S = 0$.

The *blocked* State   This is a special state where the switch is closed, which allows the submodule to be fully disconnected from the converter. This allows the converter to disable certain submodules when they are not operable, which adds to the robustness of the system.
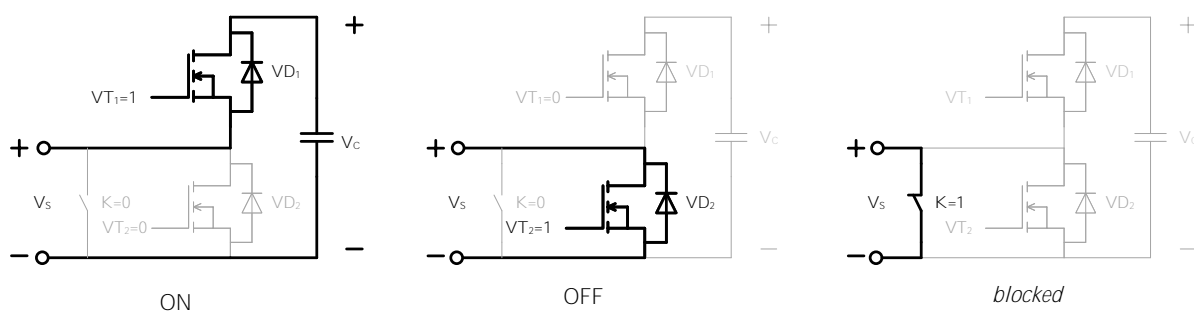
Figure 2.19   Different working states of a single MMC submodule.

14

Table 2.4   Working States of A Submodule with Different VT$_1$ and VT$_2$

State	VT$_1$	VT$_2$	K	V$_{out}$
*	0	0	0	*
OFF	0	1	0	0
ON	1	0	0	V$_C$
*	1	1	0	0
blocked	*	*	1	V$_C$

2.9.2   Nearest Level Control

Principles

Figure 2.20 shows a single-phase MMC topology. By KVL, the phase voltage u_j should satisfy

$$u_j = \frac{U_{dc}}{2} - u_{pj} - L\frac{di_{pj}}{dt} - Ri_{pj} \tag{2.2}$$

$$u_j = -\frac{U_{dc}}{2} + u_{nj} - L\frac{di_{nj}}{dt} - Ri_{nj} \tag{2.3}$$

solving which will give

$$u_j = \frac{u_{nj} - u_{pj}}{2} - \left(\frac{L}{2}\frac{di_j}{dt} + \frac{Ri_j}{2}\right). \tag{2.4}$$

Eq. (2.4) illustrates the linear relationship bewteen u_j and the difference between the two bridges, $u_{nj} - u_{pj}$. As the line inductance L is fairly small, the effect of induced current can be ignored. Hence, $u_{nj} - u_{pj}$ should be controlled respecting to the phase voltage u_j.

Assume we have some ways to keep the voltage across the capacitor, U_{SM}, constant. At some time, the number of submodules inserted to the circuit on the positive bridge is N_{pj}, and the negative bridge N_{nj}. The output voltage U_{dc} can be written as

$$U_{SM}\left[N_{pj} + \left(-N_{nj}\right)\right] = U_{dc}. \tag{2.5}$$

The total number of submodules inserted should be constant,

$$N = N_{pj} + N_{nj}. \tag{2.6}$$

Solving Eq. (2.4) (2.5) and (2.6) yields

$$N_{pj} = \frac{N}{2} - \text{round}\left(\frac{u_j}{U_{SM}}\right) \tag{2.7}$$

$$N_{nj} = \frac{N}{2} + \text{round}\left(\frac{u_j}{U_{SM}}\right). \tag{2.8}$$

Hence, the goals of the control algorithm are

1. Keep voltage across capacitors U_{SM} constant.
2. Keep number of submodules inserted on the bridges satisfying Eq. (2.7) and (2.8).
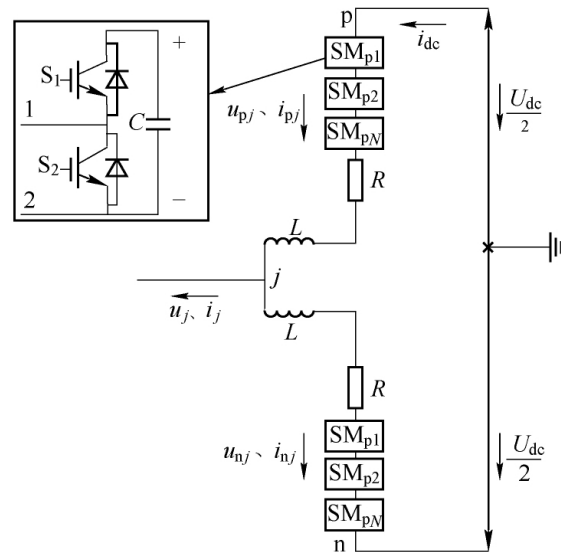
Figure 2.20   The single-phase MMC topology [12, Fig. 1].

Control Algorithm

Based on the principles discussed in §2.9.2, we raised an algorithm that maintains U_{SM}. Noted that the actual voltage across the capacitors, u_{SM}, shall not be constant as the circuit involves AC components. Hence when choosing the specific submodules to insert, the circuit should try to charge and discharge the capacitors accordingly. Note that when the bridge current $i_j > 0$, the capacitors that in the ON state will be charged, and vice versa. So the priority of SM that should be inserted is of ascend order according to the Voltage U_{SM} of each SM when $i_j > 0$. And of descend order when $i_j < 0$.

The number of submodules inserted on the positive and negative bridges should be calculated according to Eq. (2.7) and (2.8), which is already determined. The control algorithm is demonstrated in Algorithm 1.

Algorithm 1: Nearest Level Control Algorithm

Input: The phase voltage u_j, the number of submodules N, the voltage across each submodule U_{SM}, the bridge current i_j.

Output: The PWM signal for the positive and negative bridges PWM_p, PWM_n.

if $i_j > 0$ **then**

$\quad\Big|\quad$ Id_p = Index of upper submodules in ascending order according to U_{SM};

else

$\quad\Big|\quad$ Id_n = Index of lower submodules in descending order according to U_{SM};

$N_{pj} = \frac{N}{2} - \text{round}\left(\frac{u_j}{U_{SM}}\right)$;

$N_{nj} = \frac{N}{2} + \text{round}\left(\frac{u_j}{U_{SM}}\right)$;

for $i = 1$ **to** N **do**

$\quad$ **if** $i \leq N_{pj}$ **then**

$\quad\quad$ $PWM_p(Id_p(i)) = 1$;

$\quad$ **else**

$\quad\quad$ $PWM_p(Id_p(i)) = 0$

$\quad$ **if** $i \leq N_{nj}$ **then**

$\quad\quad$ $PWM_n(Id_n(i)) = 1$;

$\quad$ **else**

$\quad\quad$ $PWM_n(Id_n(i)) = 0$;

return PWM_p, PWM_n;

Algorithm 2: Simplified Nearest Level Control Algorithm

Input: The phase voltage u_j, the number of sub-modules N, the voltage across each sub-module U_{SM}, the bridge current i_j.

Output: The PWM signal for the positive and negative bridges PWM_p, PWM_n.

for $i = 1$ **to** N **do**

$\quad$ **if** $u_j \leq 0$ **then**

$\quad\quad$ $PWM_p(Id_p(i)) = 1$;

$\quad\quad$ $PWM_n(Id_n(i)) = 0$;

$\quad$ **else**

$\quad\quad$ $PWM_p(Id_p(i)) = 0$;

$\quad\quad$ $PWM_n(Id_n(i)) = 1$;

return PWM_p, PWM_n;

However, in practice, as the team only has two MMC units on a signal positive and negative bridge, the control algorithm can be simplified. The simplified control algorithm greatly reduces the scale and complexity of the circuit while maintaining the basic principles and extra voltage ripple $V_{rp} \leq 3\%$. The differences between the simplified and the original control algorithm will be discussed in the verification section §3.1.2. The simplified control algorithm is demonstrated in Algorithm 2.

3   Verification

3.1   MMC Module

3.1.1   Stability

In this subsubsection, we describe the stability test conducted on a single MMC unit. The test involved subjecting the MMC cell to a continuous load of 6 A for a duration of 30 minutes. This load test was performed at three different voltage levels for the negative terminal: -12V, 12V, and 0V.

During the test, we closely monitored the MMC unit for any signs of overheating or malfunction. Notably, the results indicated that there was no significant heating or abnormalities observed throughout the entire duration of the test. This suggests that the MMC unit exhibits good stability under prolonged and varying voltage conditions.

The photos of the test setup and the results are shown in Figure 3.1.

3.1.2   Overall System

The overall system is verified by the simulation results and the experimental results. The simulation results are also demonstrated to show the validity of the select control algorithm.

Simulation Results

The team built an MMC AC-DC converter model under regular control algorithm using Simulink, and took the following parameters at Table 3.1.

As is shown in Figure 3.3 our control algorithm could produce correct output voltage with ±1.1 V ripple, which satisfies our design specification. The voltage across SM capacitors, U_{SM}, remains almost constant at 3.9 V with a ripple ±1 V. Those results indicate that our proposed solution for NLC could work properly.
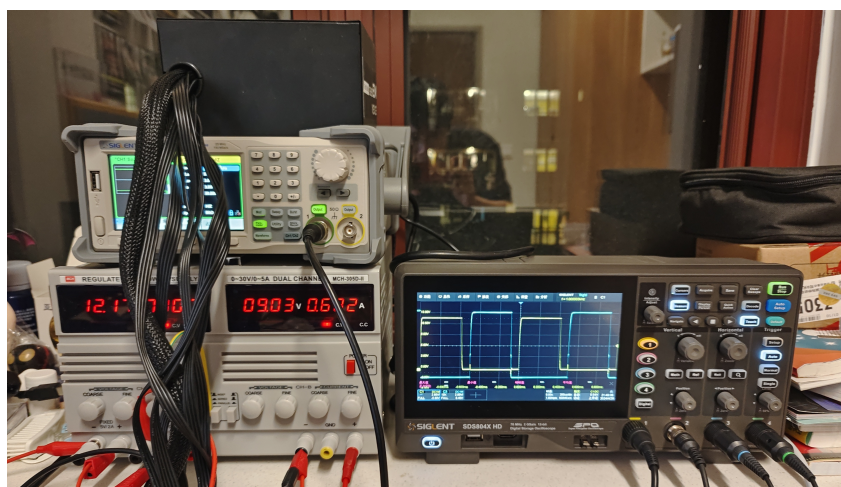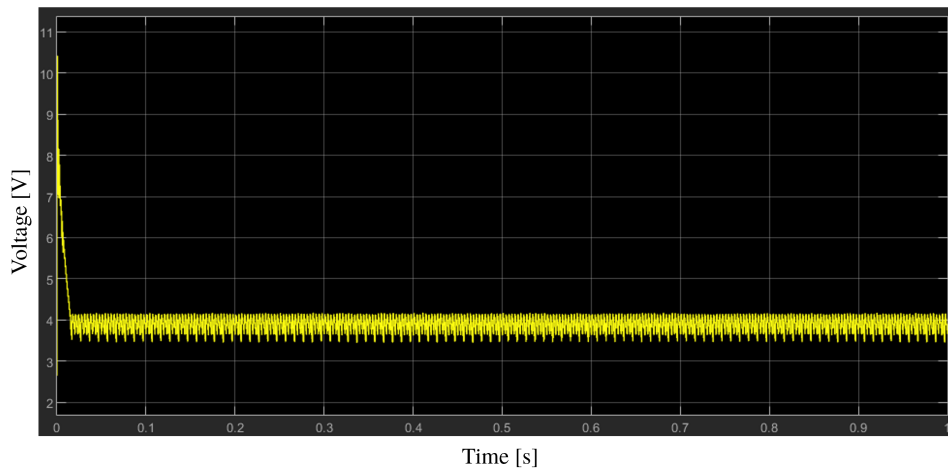

Figure 3.1   The MMC Unit Stability Test.

Table 3.1   Parameters of the Model in Simulink

Item	Parameter
AC Input	20 V, 10 Hz
Desired SM Capacitor Voltage	4 V
Desired Output Voltage	12 V

Submodule Capacitor Voltage U_{SM}

Figure 3.2   The MMC capacitor voltage.

The team also built an MMC AC-DC converter model under simplified control algorithm using Simulink, and took the same parameters as in Table 3.1.

The output waveform shown in Figure 3.4 indicates that the simplified control algorithm could produce the correct output voltage with a ripple of ±1.2 V, which satisfies our design specification.

Experimental Results

Our experimental results confirmed the predictions of these simulational results. "We simulated the conditions that were in this model on our benchtop setup," he says. The real-time measured output voltage and capacitor voltage are listed and the actual results were consistent with the simulation.

This means that when we apply the same input to the MMC AC-DC converter as we do in our simulation the regular control algorithm achieves an output voltage with a ripple of around ±1.1 V and simplified control's ripple is slightly larger, approximately ±1.2 V. These values are well within our
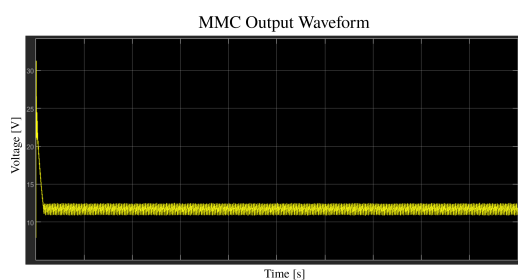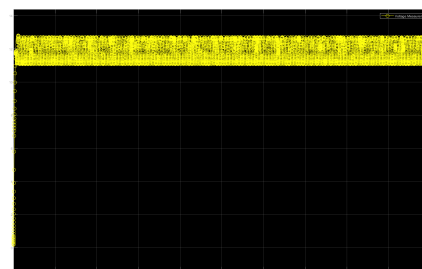

Figure 3.3   The MMC output voltage.

Figure 3.4   The MMC output voltage under simplified control algorithm.

Figure 3.5   The MMC Experimental Waveform.

acceptable limits as defined in the initial design spec.

The photos of the test results are shown in Figure 3.5.

Furthermore, the stability test conducted on the MMC unit confirmed the simulation results. The unit exhibited no signs of overheating or malfunction during the prolonged load test, indicating its robust performance under varying voltage conditions.

3.1.3   Discussion

Our comprehensive verification process, which includes both simulations and real-world experimental evaluations, has instilled confidence in the effectiveness and stability of our MMC AC-DC converter design. The findings demonstrate that both our regular and simplified control algorithms effectively achieve the desired output voltage with minimal ripple, thus meeting essential performance standards.

Effective dead time compensation at critical circuit nodes significantly reduces delays and distortions, which optimizes the converter's performance. This improvement is evidenced by the consistent and precise output voltage readings captured during both simulations and empirical tests.

The stability test on the MMC unit highlights the design's robustness, showcasing its capacity to endure prolonged operation under varied voltage conditions without abnormalities. This characteristic is crucial for ensuring the reliability and longevity of the converter in practical applications.

In conclusion, our verification process has successfully validated the performance of the MMC AC-DC converter, paving the way for its potential use in various power electronics applications. Future work could involve further refining the control algorithms and exploring the converter's performance under more extreme conditions.

3.2   Power Router

For the sensors, we also use the multimeter to test the sensors. We tested the input of the sensors, and the output of the sensors. The result is not really accurate, but it is acceptable, because in our screen our significant numbers only go to two decimal places. The following table is the comparison of the real value and the measured value.

	Input Value	Output Value	Error
MMC voltage	6.37	0.63	0.09
Back-up voltage	12.17	2.62	0.14
MMC current	5.67	5.42	0.04
Back-up current	4.94	4.61	0.07

Table 3.2   The compare of the real value and the measured value

Here we use voltage divider, so the output voltage for the MMC is calculated by the formula $V_{out} = \frac{R_2}{R_1+R_2} \times V_{in} = \frac{1}{11} \times V_{in}$. And the output voltage for the back-up is calculated by the formula $V_{out} = \frac{R_2}{R_1+R_2} \times V_{in} = \frac{1}{5.4} \times V_{in}$.

3.3 Controller

Two aspects of the controller functionalities are verified, the speed of power monitoring task, and the accuracy of on-chip ADC.

Figure **??** shows the bench settings of ADC accuracy test. The motherboard is supplied with an external 3.3 V power supply, and a DC power supply is connected to an analog input channel. The software is set to display actual ADC results to the LCD. Apply some voltage to the ADC channel and the ADC conversion results can be collected by looking at the LCD. Figures 3.6, **??**, 3.8 and 3.9 demonstrates the test results which indicates an error within ±1.5%.
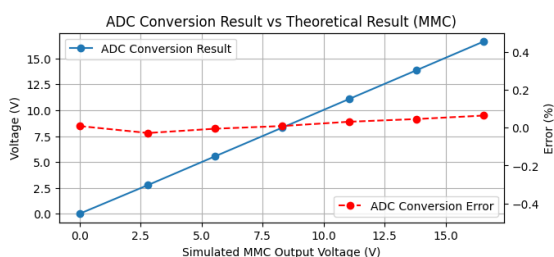
Figure 3.6   Test results of MMC voltage sensor.   **Figure 3.7**   Test results of backup power source voltage sensor.
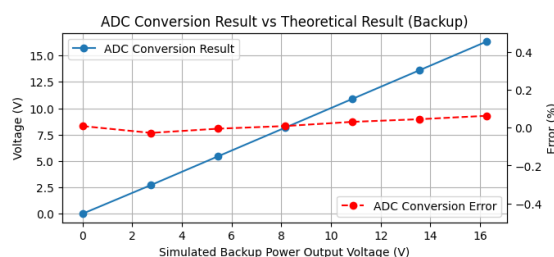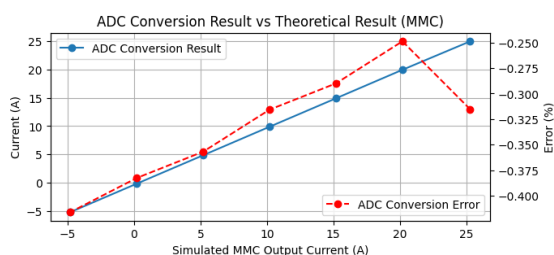
Figure 3.8   Test results of MMC current sensor.   **Figure 3.9**   Test results of backup power source current sensor.
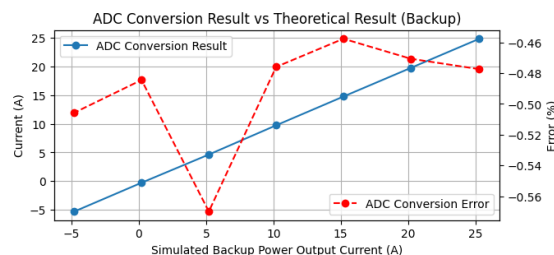
It is also vital to know the sampling rate of the power monitor task since this decides the sensitivity of the power routing functionality. To measure the average sampling rate, modify the power monitor task to allow it to print a message to the PC host through UART1 each time before reading ADC value. Test shows the MCU sends string "`ADC Read`" every 101 ms on average, indicating a sampling rate of

9.9 Hz. Such a sampling rate ensures the timely action of overload protection and power source switching.

3.4   The APP

First we test the hint and the warning in the APP. We input the wrong data and use the MQTT server to send the "No response" message, see whether the APP can show the warning. The result the APP can show the warning. We can see the receive and send status in the APP and MQTT server sides.

Figure 3.10   The warning in the APP.

Figure 3.11   The send status in the APP.

Furthermore, we also check the link and QR code in the APP, which is also successful, leading us to the website. And the music player in the APP also works well, we can play the music and stop the music at the right time.

4   Conclusion

4.1   Cost Analysis

4.1.1   Labor Cost

According to [13], the estimated labor cost of each partner of the team can be calculated by
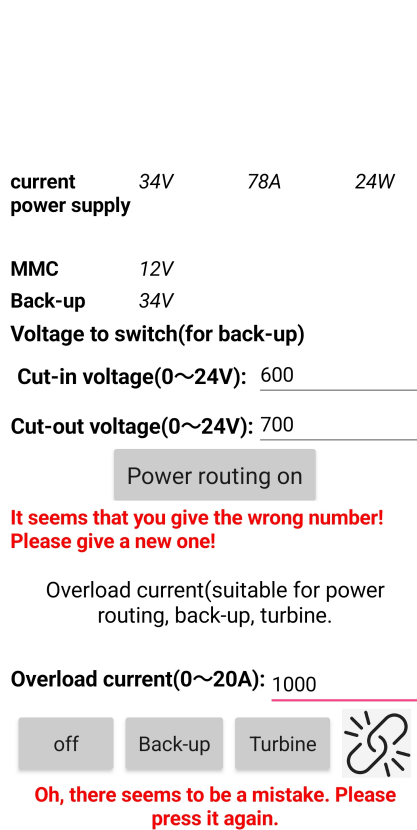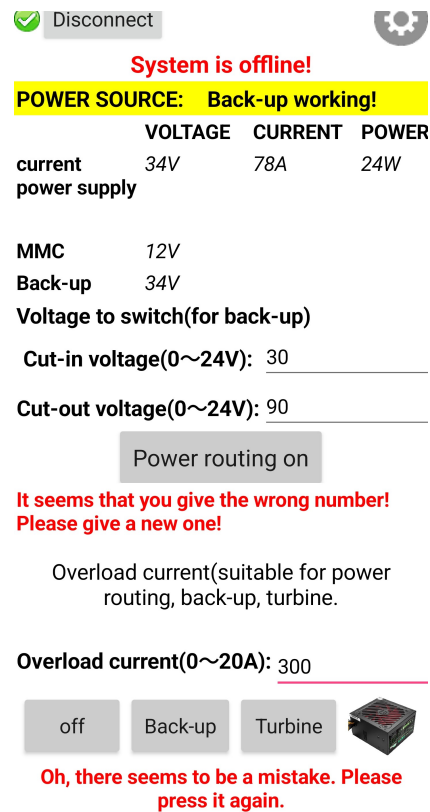
$$E = 2.5S \cdot T \tag{4.1}$$

where S is the ideal salary per hour and T is the actual hours spent on the project. According to the TA salary at ZJUI in 2022, it is possible to assume $S = ¥50$ yuan/h. The project lasts 11 weeks, and each person has to work 4 hours a day, 6 days a week, which is $T = 4 \times 6 \times 11$ hours throughout the semester. This gives

$$E = 2.5 \times 50 \times 264 = ¥33\,000.00 \text{ yuan/person.} \tag{4.2}$$

4.1.2   Material Cost

As the PCB design has not been finalized, the following cost analysis table (Table 4.1) should only be taken as an estimation. The total financial cost of this project should be $33000 \times 3 + 1713.84 = ¥100\,713.84$.

Table 4.1   Estimated Material Cost Analysis Table

Item	Price per Unit (CNY)	Amount	Subtotal (CNY)
Wind Turbine (24V200W)	670	1	670
ATK STM32F103 Core Board Dev. Kit	297.16	1	297.16
ATK ESP8266D WiFi MCU Module	22.82	1	22.82
Support Rod of Wind Turbine	100	1	100
Panic Button (Taibang)	4	1	4
Panic Button (CHNT)	6.8	2	6.26
ACS712 Current Measuring Module	8.36	1	13.6
DSP28377 Dev. Kit (from lab)	0	1	0
Wires	3.27	4	13.08
PCB Manufacturing and Components	200	3	600
		Total	**¥1 726.89**

4.1.3   Mass Production Estimation

For mass production, the MCU minimum system board is no longer needed; instead, the STM32F103 MCU can be directly integrated into the main PCB. This also applies to ESP8266 WiFi MCU and DSP28377 MCU. The support rod of the turbine could be cheaper, as mass production of such metal components can be done using automatic machines which is cheaper. Assume 1000 sets can be sold

throughout the lifecycle of the product, the labor cost in development distributed to each set will be ￥100.71. The following Table 4.2 should apply.

Table 4.2   Estimated Mass-Production Cost Analysis Table

Item	Price per Unit (CNY)	Amount	Subtotal (CNY)
Wind Turbine (24V200W)	670	1	670
STM32F103 MCU	15	1	15
ESP8266 WiFi MCU	4.8	1	4.8
Support Rod of Wind Turbine	80	1	80
Panic Button (Taibang)	4	3	12
DSP28377 MCU	150	1	150
PCB Manufacturing and Components	200	1	200
Human Resource in Product Development			100.72
		Total	**￥1 232.52**

4.2   Safety

Safety is always the top priority when it comes to the design of physical systems. As this project involves electrical and mechanical parts, the safety of the surroundings of the system is important. To ensure safety within the development process and the throughout lifecycle of the product, it is vital to keep the following requirements satisfied:

1. Keep clear of the wind turbine whenever it is unlocked and can rotate freely to avoid any people being hurt by the rotating turbine. Safety distance of the turbine is set to 2 m.
2. Keep the circuit well enclosed within water-resistant containers whenever the generator system is applied in any outdoor environment.
3. All power transmission lines within the generator system should be properly fused to avoid fire triggered by overheat.
4. All subsystems related to rechargeable battery use should comply with "Safe Practice for Lead Acid and Lithium Batteries" [14], and the customized battery charger should comply with "Household and similar electrical appliances – Safety – Particular requirements for battery chargers" (GB 4706.18-2014) [15].
5. All wires and devices that have current and/or voltage exceeding the limit set by China National Standard "Extra-low voltage (ELV) – Limit values" (GB/T 3805-2008) [16] should be kept unreachable by the surroundings unless they are unconnected to power.
6. The generator system should comply with the following China National Standards:

   (a) "Household And Similar Electrical Appliances – Safety – Part 1: General Requirements" (GB 4706-2005) [17].

   (b) "Generator of Small Wind Turbines – Part 1: Technical Condition" (GB/T 10760.1-2017) [18].

4.3   Ethics

Ethical considerations are vital to a successful product design. The development of the project should strictly follow "IEEE Code of Ethics" [19], and the team will devote themselves to upholding integrity, responsibility, and professionalism. The product should not convey discrimination towards any person or group, and be kept from injuring any surroundings.

In detail, the following requirements should be remembered during and after the senior design project:

1. The "IEEE Code of Ethics" [19] especially mentions that the engineers should "hold paramount, the safety, health, and welfare of the public," which is vital to the success of this project. The safety and health of any person or animal involved in this project should be ensured. For this project, the turbine should be kept from injuring any animals like birds that fly by, and any people around. Careful check is necessary before unlocking the turbine and starting the system to ensure people around are aware of the rotating paddles and animals are away from the testing site.

2. Academic integrity is important to this project. During the development, any work done by another person or team that is applied to this project should be cited properly in any documents written for this course. The team should make sure the project submitted is their original work, and to "credit properly the contributions of others" [19] when presenting their work in either written form or oral form.

3. Teamwork matters. The team agrees that they will "seek, accept, and offer honest criticism of technical work" [19] to each other. Everyone in the team should be "treated fairly and with respect" [19]. The team should not discriminate against anyone either in or out of the team.

4. Compliance. The development process and the product itself should comply with relevant laws and national standards mentioned in section 4.2. The purchase of any materials needed for the project should be properly recorded and archived for further investigation of expenditures.

References

[1] National Energy Administration. "国家能源局发布 2023 年全国电力工业统计数据 [NEA releases national power industry statistics for 2023]." (Jan. 26, 2024), [Online]. Available: https://www.nea.gov.cn/2024-01/26/c_1310762246.htm (visited on 01/27/2024).

[2] ARM Ltd. "Introduction," CMSIS-FreeRTOS Version 10.5.1. (Dec. 1, 2022), [Online]. Available: https://arm-software.github.io/CMSIS-FreeRTOS/latest/ (visited on 03/22/2024).

[3] Espressif, *ESP8266EX 技术规格书 [ESP8266EX Technical specifications]*, ESP8266EX Datasheet, Jun. 2023. [Online]. Available: https://www.espressif.com.cn/sites/default/files/documentation/0a-esp8266ex_datasheet_cn.pdf (visited on 03/18/2024).

[4] Espressif. "AT 命令集 [AT Instructions set]," ESP-AT 用户指南 [ESP-AT User Manual]. (2020), [Online]. Available: https://espressif-docs.readthedocs-hosted.com/projects/esp-at/zh-cn/release-v2.2.0.0_esp8266/AT_Command_Set/index.html (visited on 03/18/2024).

[5] EMQ Technologies Inc. "EMQX: The World's #1 Open Source Distributed MQTT Broker," EMQX. (n.d.), [Online]. Available: https://www.emqx.io/ (visited on 03/19/2024).

[6] "MQTT: The Standard for IoT Messaging," MQTT.org. (n.d.), [Online]. Available: https://mqtt.org/ (visited on 03/19/2024).

[7] Massachusetts Institute of Technology. "About Us." (n.d.), [Online]. Available: https://appinventor.mit.edu/about-us (visited on 03/11/2024).

[8] "AI2 MQTT extension: Sensor readings back and forth," Ullis Roboter Seite. (Nov. 17, 2020), [Online]. Available: https://ullisroboterseite.de/android-AI2-PahoMQTT-en.html (visited on 03/27/2024).

[9] M. N. Raju, J. Sreedevi, R. P Mandi, and K. Meera, "Modular multilevel converters technology: A comprehensive study on its topologies, modelling, control and applications," *IET Power Electronics*, vol. 12, no. 2, pp. 149–169, 2019. [Online]. Available: https://onlinelibrary.wiley.com/doi/abs/10.1049/iet-pel.2018.5734.

[10] E. N. Abildgaard and M. Molinas, "Modelling and control of the modular multilevel converter (MMC)," *Energy Procedia*, Technoport 2012 - Sharing Possibilities and 2nd Renewable Energy Research Conference (RERC2012), vol. 20, pp. 227–236, Jan. 1, 2012, ISSN: 1876-6102. DOI: 10.1016/j.egypro.2012.03.023.

[11] Shuai Liang, "应用于退役动力电池储能电站的 MMC 控制策略研究 [Research on MMC control strategy applied to decommissioned power battery energy storage plant]," M.Eng. Thesis, Lanzhou University of Technology, Lanzhou, 2023. DOI: 10.27206/d.cnki.ggsgu.2023.000267.

[12] L. Zheng, J. Xu, and S. Ma, "一种改进的 MMC 电容电压均衡控制方法 [An improved control method for MMC capacitor voltage balancing]," *Journal of Beijing Jiaotong University*, vol. 41, no. 2, pp. 112–116+122, 2017. [Online]. Available: https://kns.cnki.net/kcms2/article/abstract?v=xz5HP63VF6ckRnnHNgkPy7OwF8DkOIVnqsyV2gcGAz2a062H9aKKrtymeeftM91tU7T_npgSaHHtlvGF8VL645hWAA6SdQcSDmUA1vcdNhqL8qHoe8VoEXVRQXWS_ObcTdfbuweEKcT6XwtFEHgqWw==&uniplatform=NZKPT&language=CHS.

[13] Staffs of ECE 445 and ECE Editorial Services, *Preparing your final report for ECE 445, senior design*, University of Illinois at Urbana-Champaign, Sep. 2019. [Online]. Available: https://cours es.grainger.illinois.edu/ece445zjui/documents/ECE_445_Final_Report_Guidelines.pdf (visited on 03/22/2024).

[14] ECE 445 Spring 2016 Course Staff, *Safe practice for lead acid and lithium batteries*, University of Illinois at Urbana-Champaign, Apr. 13, 2016. [Online]. Available: https://courses.grainger.illi nois.edu/ece445zjui/documents/GeneralBatterySafety.pdf (visited on 02/27/2024).

[15] Ministry of Industry and Information Technology, 家用和类似用途电器的安全，电池充电器 的特殊要求 *[Household and similar electrical appliances – Safety – Particular requirements for battery chargers]*, GB 4706.18-2014, Dec. 5, 2014, [Online]. Available: https://openstd.samr .gov.cn/bzgk/gb/newGbInfo?hcno=674F4507CC2ACFAD9F0C6C85895DD64E (visited on 02/12/2024), Active.

[16] Standardization Administration of China, 特低电压 (ELV) 限值 *[Extra-low voltage (ELV) – Limit values]*, GB/T 3805-2008, Jan. 22, 2008, [Online]. Available: https://openstd.samr.gov.cn/bzg k/gb/newGbInfo?hcno=2A3598C5E4A0EB6BDBD6D1BD52681A6A (visited on 02/29/2024), Active.

[17] Ministry of Industry and Information Technology, 家用和类似用途电器的安全，第 1 部分：通 用要求 *[Household and similar electrical appliances – Safety – Part 1: General requirements]*, GB 4706.1-2005, Aug. 26, 2005, [Online]. Available: https://openstd.samr.gov.cn/bzgk/gb/new GbInfo?hcno=EBFC09A41682AC72F3F5216DBA619A40 (visited on 02/12/2024), Active.

[18] China Machinery Industry Federation, 小型风力发电机组用发电机，第 1 部分：技术条件 *[Generator of small wind turbines – Part 1: Technical condition]*, GB/T 10760.1-2017, Oct. 14, 2017, [Online]. Available: https://openstd.samr.gov.cn/bzgk/gb/newGbInfo?hcno=5517004881 FF78E39396E316AE2114CC (visited on 02/11/2024), Active.

[19] IEEE Board of Directors, *IEEE code of ethics*, Institute of Electrical and Electronics Engineers, Jun. 2010. [Online]. Available: https://www.ieee.org/content/dam/ieee-org/ieee/web/org/about/c orporate/ieee-code-of-ethics.pdf.

Appendix A   Requirement and Verification Tables

Table A.1   Requirements and Verification Table of the MMC

ID	Requirement	Verification
1	The MMC could generate DC output with ripple smaller than ±10%.	Observe the output voltage through DMM, the LCD screen on the controller, or the mobile app.

Table A.2   Requirements and Verification Table of the Power Router

ID	Requirement	Verification
1	The four relays receive signals from the control part and choose the break-make of the MMC and back-up battery.	Give the signal to each relay and check the connection of the four circuit.
3	The power router receive the signals from the system control and choose which should be connect to the load.	Send signals to the two input of power router, check if it can change which power supply to the load(Here we can use an oscilloscope.) in 0.1 ms.

Table A.3   Requirements and Verification Table of the Remote User Interface

ID	Requirement	Verification
1	The app can connect to the MQTT broker.	Enter broker IP and credentials and check the dashboard of the broker server if the client is connected.
2	The app can display real-time system information.	Run the system and connect output to the Digital Multimeter (DMM). Check if (1) the app shows real-time power information (current power source, picture, and voltage-current-power), and (2) the displayed information matches the DMM.

Table A.3   Requirements and Verification Table of the Remote User Interface

ID	Requirement	Verification
3	The app can remotely start the system by tapping the "off", "back-up", "turbine" and "power routing" buttons. The "power routing" can let power change at the adjustable voltage, the "turbine" button will let MMC connect to the load, "back-up" button will connect the back-up power to the load.	Tap the four buttons and check if the system output produces correct result.
4	The app can adjust the cut-in and cut-off voltage for the back-up power, and the overload current for the system.	Change the value of the cut-in and cut-off voltage and overload current, check if the system can produce the correct result.
5	The cut-in and cut-off voltage vary from $0\,\mathrm{V}$ to $24\,\mathrm{V}$, and the overload current varies from $0\,\mathrm{A}$ to $20\,\mathrm{A}$. The cut-in voltage should be less than the cut-off voltage. If you give the wrong value, you will receive the warning.	Change the value of the cut-in and cut-off voltage and overload current, check if the system can produce the correct result.
6	The app have a about page, which can show the QR code and link to the website of our group.	Tap the about button, check if the app shows the correct information.

Table A.4   Requirements and Verification Table of the System Controller and Local User Interface

ID	Requirement	Verification
1	The system displays voltage and current info from VCMU at a frequency of 1 Hz.	Visually check the LCD output.

Table A.4 Requirements and Verification Table of the System Controller and Local User Interface
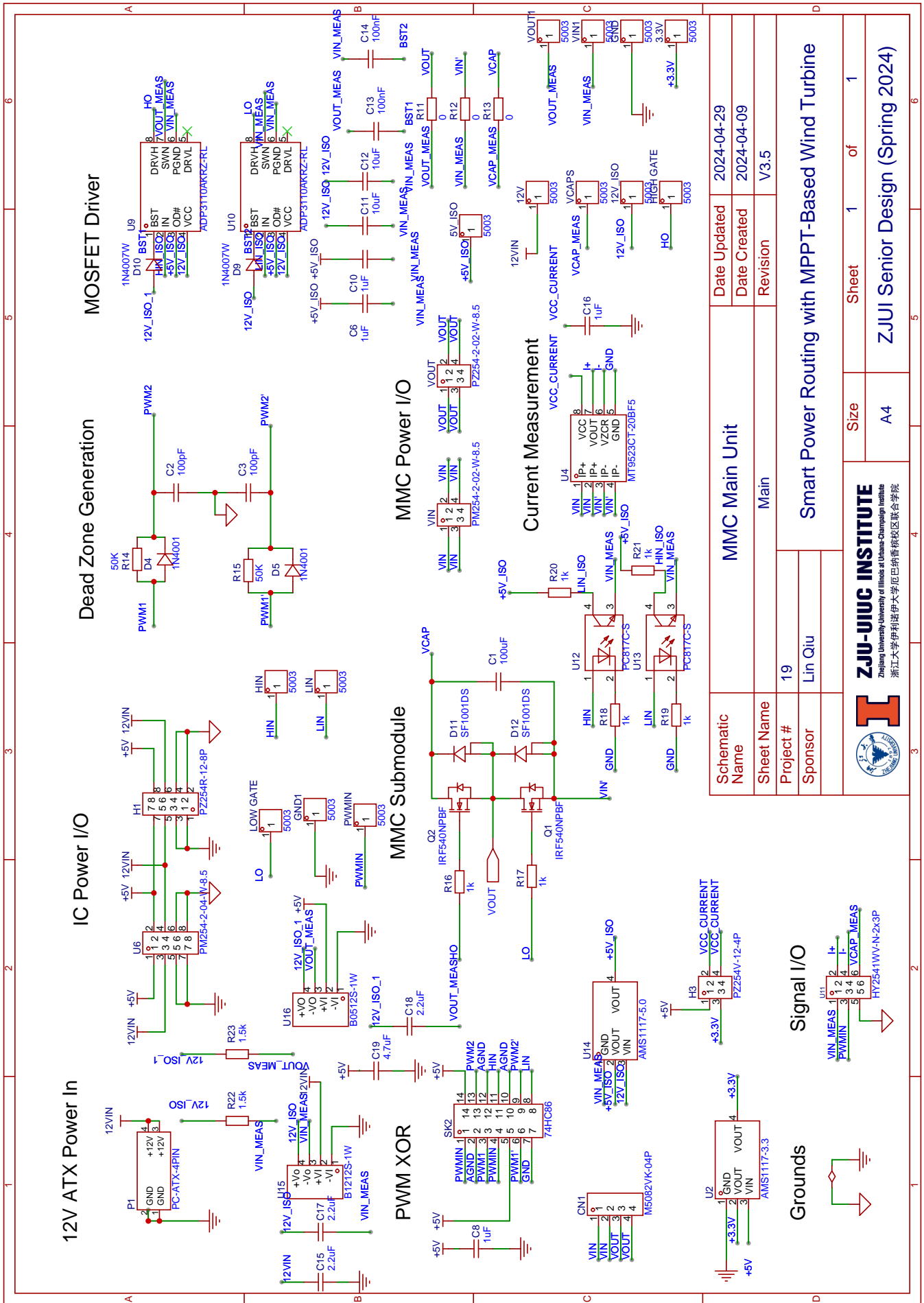
ID	Requirement	Verification
2	The controller shall send a power-off signal to the router if the current delivered exceeds the maximum current toleration (specified by user, but less than 20 A) for more than 1 s.	Specify a proper current limit. Cut in the load and check if the output is cut-off under the specified scenario.
3	The controller shall send a signal to the router to switch the output to the backup source if the MMC fails to deliver sufficient power.	Set the specified cut-in and cut-out voltage on mobile and check if the router works properly.
4	The controller shall control LEDs on the control panel to indicate system status and provide visual warnings.	Inspect LED behavior when powering on the system, changing the output power source, connecting/disconnecting wireless network and simulating overload scenarios to ensure they accurately represent system status and provide visual warnings.

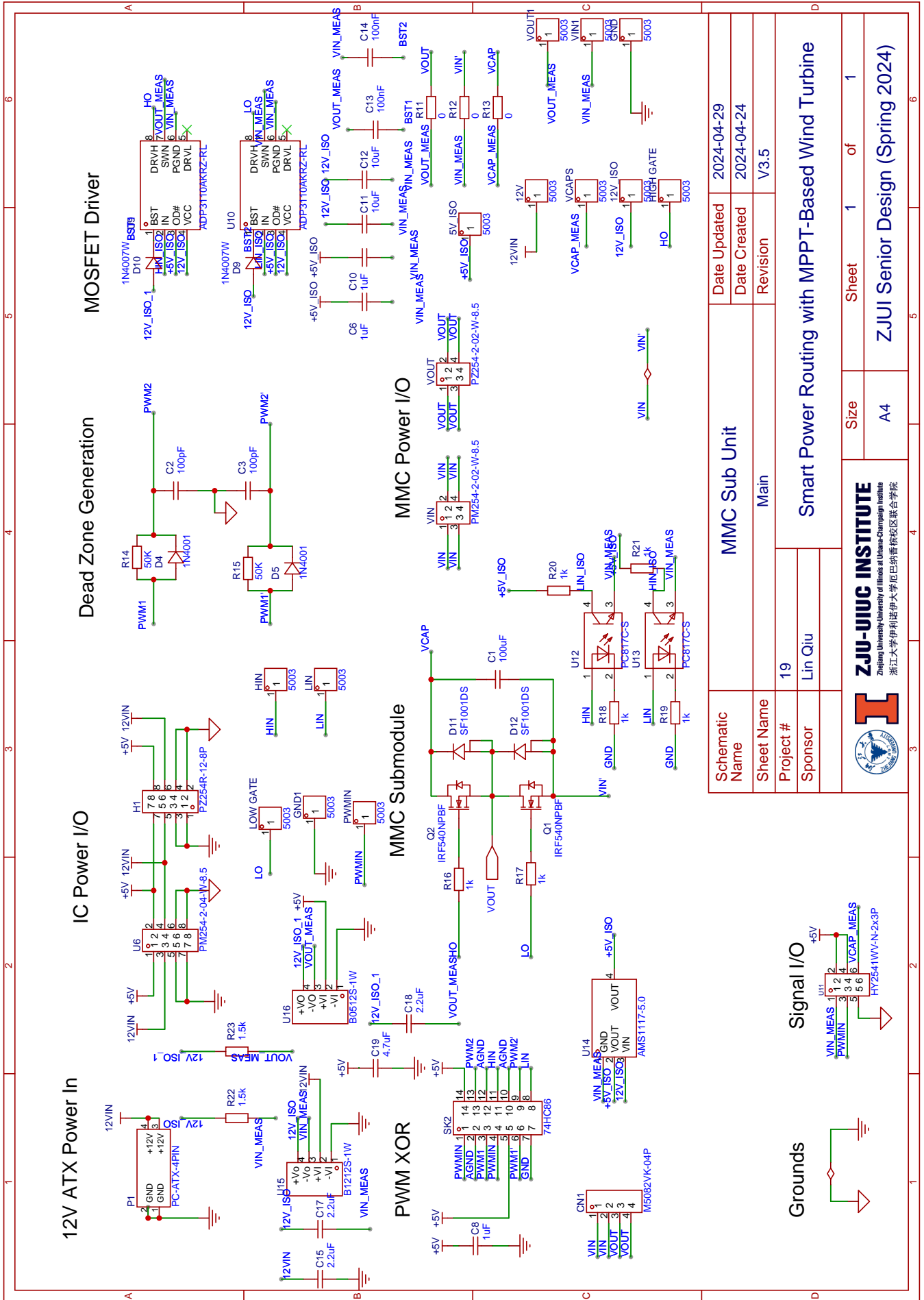**Table A.5** Requirements and Verification Table of Wireless Communication

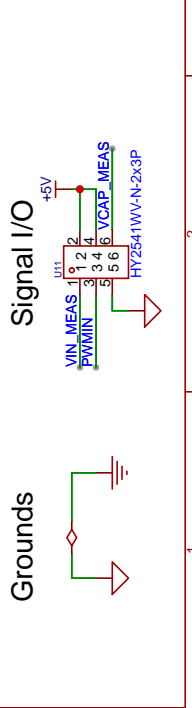| ID	Requirement	Verification
1	The module should connect the MQTT server successfully.	Start the MQTT server and send AT instructions from the system controller. Check if the EMQX Dashboard shows an active connection from ESP-12F.
2	The module sends payload based on instructions from the system controller.	Program the system controller and let the module publish a test message to a test topic. Check if another MQTT client on PC can receive the message.
3	The module automatically reconnects the MQTT server when the connection fails.	After a stable connection to the MQTT server is established, turn off the MQTT service on the server and restart it 2 s later. Check if the connection is recovered within 5 s.
4	The module automatically reconnects the WiFi Access Point when the connection fails.	After a stable connection to the Acess Point is established, turn off the Acess Point and restart it 1 s later. Check if the connection is recovered.

Appendix B   Design Schematics

In the following pages, the hardware schematics will be presented.

Smart Power Routing with MPPT-Based Wind Turbine

MMC Main Unit

Schematic Name	Main	Size	A4
Sheet Name			
Project #	19	Date Updated	2024-04-29
Sponsor	Lin Qiu	Date Created	2024-04-09
		Revision	V3.5
		Sheet	1 of 1

ZJUI Senior Design (Spring 2024)

ZJU-UIUC INSTITUTE
Zhejiang University/University of Illinois at Urbana-Champaign Institute
浙江大学伊利诺伊大学厄巴纳香槟校区联合学院

Smart Power Routing with MPPT-Based Wind Turbine

MMC Sub Unit

Main

ZJUI Senior Design (Spring 2024)

Date Updated	2024-04-29
Date Created	2024-04-24
Revision	V3.5

| Size | A4 |

Sheet 1 of 1

Schematic Name	
Sheet Name	
Project #	19
Sponsor	Lin Qiu

ZJU-UIUC INSTITUTE
Zhejiang University of Illinois at Urbana-Champaign Institute
浙江大学伊利诺伊大学厄巴纳香槟校区联合学院

MOSFET Driver

Dead Zone Generation

MMC Power I/O

IC Power I/O

MMC Submodule

Signal I/O

12V ATX Power In

PWM XOR

Grounds

Smart Power Routing with MPPT-Based Wind Turbine

MMC_control

P1

ZJUI ECE 445 Sp24 Project #19

Rong Li

T. Zhong, Z. Zheng

2024-05-09

2024-04-19

V1.0   A4

Batt. Power Input

Power Indicator

3V3 Regulator

HSE

STM32 UART1 to USB-C

ESP-12F UART Header (for Firmware Downloading)

2'' LCD (FPC)

LED Indicators

STM32F103 MCU

Test Points

VDDA and VSSA

ESP-12F Wi-Fi Module

Reset Buttons

Panic Button

To MMC Controller

To Power Router

SWD Debug Header

BOOT0 & BOOT1

VREF+

Voltage Measurement
(with Voltage Followers)

Current Measurement

Output

Router

From Motherboard

From Backup

Backup Power
Manual Startup

From MMC

Schematic Name	Schematic1
Sheet Name	Main
Project #	19
Sponsor	Lin Qiu

Smart Power Routing with MPPT-Based Wind Turbine

	Date Updated	2024-05-09
	Date Created	2024-05-02
	Revision	V2
Size	Sheet	1 of 1
A3	ZJUI Senior Design (Spring 2024)	

ZJU-UIUC INSTITUTE
Zhejiang University/University of Illinois at Urbana-Champaign Institute
浙江大学伊利诺伊大学厄巴纳香槟校区联合学院